

Numerical methodology for design and evaluation of natural circulation systems for MSR applications

J. S. Narváez Arrúa, A. Cammi, S. Lorenzi

Politecnico di Milano, Energy Department, Nuclear Engineering Division
via La Masa 34, 20156, Milano, Italy

jonassebastian.narvaez@polimi.it; antonio.cammi@polimi.it; stefano.lorenzi@polimi.it

P P. Rubiolo

Univ. Grenoble Alpes, CNRS, Grenoble INP, LPSC,
53, rue des Martyrs 38000 Grenoble, France

rubiolo@lpsc.in2p3.fr

ABSTRACT

This work focuses on the development of a comprehensive numerical methodology for the study of natural circulation systems using molten salts as working fluid, in particular for its application in the design of passive safety systems for Molten Salt Reactors (MSRs). The goal of the methodology is to evaluate the performance of possible 3D natural circulation configurations through the description of their dynamic behavior, with a focus in the identification of bifurcation phenomena and performing a stability analysis. The numerical tool implementing this methodology is based on a CFD-based MATLAB-OpenFOAM coupling and has been evaluated against a numerical benchmark of a differentially heated cavity, showing good agreement with literature results. For a first assessment of the performance of the tool a simple 2D case of a simple natural circulation configuration known as Rayleigh-Bénard convection has been used. This configuration results from a 2D enclosure heated and cooled from the bottom and top surfaces respectively. The dynamic states of this system have been studied for a large range of both geometric and physical parameters, showing both steady state and oscillating solutions. A bifurcation diagram is produced, showing the transition between the different solutions. In the vicinity of certain bifurcation points hysteresis phenomenon has been observed. The numerical tool developed for the evaluation of natural circulation systems has shown a good performance both for the description of the thermal-hydraulic system as well as for the stability analysis. The complexity and variety of the possible solutions for this first assessment illustrates the need of a robust and systematic methodology for the considered applications which in practice will involve more complex geometries and additional underlying phenomena.

KEYWORDS

Molten salts, natural circulation, thermal-hydraulics, CFD

1. INTRODUCTION

The use of chloride and fluoride molten salts as coolants for energy systems has been investigated for several decades because of their high heat capacity, high working temperatures, low vapor pressure and good chemical and irradiation stabilities. In recent years, its use has regained interest, mainly in energy applications either for thermal energy storage or as a heat carrier fluid for solar and nuclear energy applications [1,2].

While there is a similarity between some commonly used fluids, said water, and molten salts applications in some fundamental parameters like Reynolds and Prandtl numbers, molten salts have some important additional specific phenomena that require specific studies. Firstly, they are participative semi-transparent media and thus radiative heat transfer will take place in the bulk of a molten salt. Also, depending on the temperature, they can undergo relatively complex solidification and melting processes at high temperature. Finally for nuclear applications one can mention internal heat generation due to nuclear reactions in the case of a nuclear molten fuel salt which causes the existence of an internal heat source in the flow [3].

Due to these distinctive molten salts phenomena, a strong need for a new numerical methodologies and tools able to accurately evaluate the performance of natural circulation circuits and thus to provide early feedback for the design novel systems and components involving molten salts. This is for example the case of some Gen IV Reactors designs like the Molten Salt Fast Reactors (MSFR) that make use of passive systems based on natural circulation of molten salts for nuclear decay heat removal [4]. Indeed, the use of passive safety systems provides this reactor with the capability of having an intrinsically safe behaviour during possible accidents [4]. An example of such passive safety system is the decay heat removal system (DHRS) which makes use of natural circulation to remove decay heat, in such a way that without an active control action, a safe dynamic state is reached. It is important to note that the behaviour of natural circulation system is highly non-linear and results from a balance between the effects of the driving forces, the geometry of the system and the initial conditions for which the natural circulation is established. As the safety systems are expected to function within a certain range of possible scenarios and conditions, it is therefore necessary to consider the possible existence of bifurcation points; given sets of parameters for which the qualitative behaviour of the system changes [6]. For example, the behaviour of the system could shift from a unique dynamic state to branching into several possible states that may not even include the original one. This means that while for a particular condition the safety system would be able to achieve the expected behaviour, a small fluctuation on the conditions could potentially compromise the functionality of the system by making the original state unstable or even leading to an entirely different final state which is not acceptable.

The presence of the bifurcation phenomena does not necessarily impede the proper functioning of the system. For example, it is possible that among the newly different states the original state continues to be dominant or it is only slightly modified. The fundamental goal in the early design phase of these safety systems is therefore to assess for all the possible states the system may undergo, avoiding the type of bifurcations that could lead to unstable or undesired dynamic states.

Considering these constraints on the behavior of the system, the degree of reliability required for safety systems and the specific phenomena of molten salts, it is clear that a dedicated and systematic methodology is necessary for allowing a comprehensive description of natural circulation molten salt systems, together with a proper performance verification stage against dedicated experimental data. The present work concentrates in a preliminary formulation of such methodology, drawing the primary constraints, the models needed for the different steps, the starting point through the study of a simplified base case and the process to be followed for a progressive and systematic development to be ultimately applied for the design of a molten salt experiment.

2. METHODOLOGY FORMULATION AND NUMERICAL IMPLEMENTATION

The first step of the work begun with the careful numerical modeling of the thermal-hydraulic natural circulation system selected for the implementation of the methodology. Starting from this numerical model and for a given configuration, the different operational conditions can be evaluated by progressively covering the specific range of interest of the governing parameters. This constitutes a straightforward method for obtaining the different possible solutions of the system. This direct method allows finding the locations of the bifurcation points as the set of parameters that limit the ranges where there are several coexisting solutions. Afterwards, this process is followed by the execution of an analysis to evaluate the feasibility of the obtained solutions in terms of stability. This direct method allows obtaining, within the studied range of parameters, the operational conditions of the system that give a solution with the desired dynamic and stability. It is important to note, that this direct analysis method is practical only for relatively simple system since it would require excessive computational resources in more realistic geometries.

2.1. Description of the Thermal-hydraulic System

The description of the thermal-hydraulic system is achieved through the resolution of the coupled equations of mass, momentum and energy. Additionally, for the expected conditions found in our applications, due to the relatively low velocity of the fluid and the absence of high temperature gradients, the flow can be considered as incompressible, allowing as well the use of Boussinesq approximation for buoyant flows. The resulting governing equations are then:

$$\nabla \cdot U = 0 \quad (1)$$

$$\frac{\partial U}{\partial t} + (U \cdot \nabla)U + \nabla p^* - \nabla[\nu D(U)] = \frac{\rho(T)}{\rho_{ref}} g, \text{ with } \rho(T) = \rho_{ref}[1 - \beta(T - T_{ref})] \quad (2)$$

$$\frac{\partial T}{\partial t} + (U \cdot \nabla)T - \nabla \cdot (\alpha \nabla T) = 0 \quad (3)$$

In Eqs. (1)–(3), U represents the velocity vector, T stands for the temperature, and p is the pressure divided by a reference density ρ_{ref} . $\rho(T)$ corresponds to the actual value of the density in the system, ν represents the kinematic viscosity, g is gravity acceleration vector, and α is the thermal diffusivity. The operator denoted as D stands for $D(U) = (\nabla U + \nabla^H U)/2$, where the superscript H indicates the transpose.

The implementation for this model is carried out using the open source library software OpenFOAM® [7], which is based in the Finite Volume Method (FVM) C++ library, used for continuum mechanics and fluid dynamics simulations. The current capabilities of this software allow the resolution of this problem decreasing the numerical development effort.

2.2. Stability Analysis Procedure

For the stability analysis an initial model based on Linear Stability Theory (LST), known as modal analysis, is used to evaluate the asymptotic stability of the system, according to the Lyapunov criteria [8]. Starting from an equilibrium state, obtained as previously described, the system is considered asymptotically stable only if after being subjected to a perturbation the original condition is recovered after an infinite time. The first step considers a division between the equilibrium state, referred to as the base solution (q_0), and a small unsteady perturbation around it ($dq \ll q_0$). By reworking the equations with this definition of the variables and neglecting the terms with order greater than one, a linearized set of equations is obtained. This new equation describes the behavior of the perturbations of the temperature (δT), pressure (δp) and velocity (δU) fields:

$$\nabla \cdot \delta U = 0 \quad (4)$$

$$\frac{\partial \delta U}{\partial t} + (U_0 \cdot \nabla) \delta U + (\delta U \cdot \nabla) U_0 + \nabla \delta p^* - \nabla \cdot [\nu D(\delta U)] + \beta g \delta T = 0 \quad (5)$$

$$\frac{\partial \delta T}{\partial t} + (U_0 \cdot \nabla) \delta T + (\delta U \cdot \nabla) T_0 - \nabla \cdot (\alpha \nabla \delta T) = 0 \quad (6)$$

where U_0 and T_0 stand for the velocity and temperature fields of the base solution respectively. Furthermore, this method studies temporal instabilities by considering a perturbation with a generic wavelike form and by making no assumptions about the homogeneity of the base solutions. Under those assumptions, the perturbations can be described as:

$$\partial q(x, y, z, t) = \hat{q}(x, y, z) e^{(\omega_r + i\omega_i)t} \quad (10)$$

where ω_r represents the amplification of the wave and ω_i is the related angular frequency. Combining this functional form of the perturbation with the linearized system, the problem is then reduced to an EigenValue Problem (EVP). The eigenvalues of the linearized operator obtained as the solution of this problem represent a group of characteristic frequencies to which the system responds preferentially. These results allow determining the stability of the asymptotic solution of the system, since if at least one the related eigenmodes of the system increases in time instead of decaying, the system equilibrium state is unstable. From Eqs. 4-6 it is important to notice that the linearized system only takes into account the base solution of the system from a single description of the temperature and velocity fields, causing this method to be only applicable for the cases with a steady-state base solution, since in the case that this exhibits an oscillatory behavior, the linearized system would be unable to capture its temporal variation.

Due to the high computational cost associated to the direct resolution of the EVP, instead a time-stepping approach is selected [9]. Moreover, adding a Dynamic Mode Decomposition (DMD) algorithm, the characteristic frequencies are retrieved using the time evolution of the linearized system. A more detailed description of this method can be found in [10].

The routine for the modal analysis, enclosing both the evolution of the linearized system and the resolution of the EVP, is implemented as a MATLAB-OpenFOAM coupling. The resolution of the base state is obtained with the implementation described in the previous subsection, while for obtaining the evolution of the linear system specific solvers were developed within the structure of OpenFOAM and the DMD algorithm is implemented in MATLAB.

2.3. Selection of Base Case: Rayleigh-Bénard Convection

Once the basic methodology has been presented, in this section the selection of a base case for the analysis implementation is presented. The first requirement for the base case is that it should exhibit bifurcation phenomena, as the detection of the bifurcations points and the analysis over the ranges with several coexisting solutions is a fundamental part of the presented methodology. In addition, the base case should also comply with some basic requirements as:

- A simple geometry and a laminar regime, to focus the analysis in the aspects of interest.
- An acceptable degree of complexity, considering that it will be used for the development of the tools that will be used more realistic and thus complex geometries.
- Availability of existing results on the case as the goal is to develop and assess the methodology and not to produce particular results for the case.

After a review of the literature concerning natural convection configurations, a specific type of natural convection case known as Rayleigh-Bénard convection was identified as a potential study case. This flow

system has indeed several levels of complexity and requires different degree of analyses for a wide range of operational conditions. A Rayleigh-Bénard convection flow is a natural convection configuration that arises when a body of fluid is contained between two parallel plates, with hot and cold fixed temperatures in the lower and upper plates respectively, as depicted in the Fig. 1, while the rest of the boundaries are adiabatic.

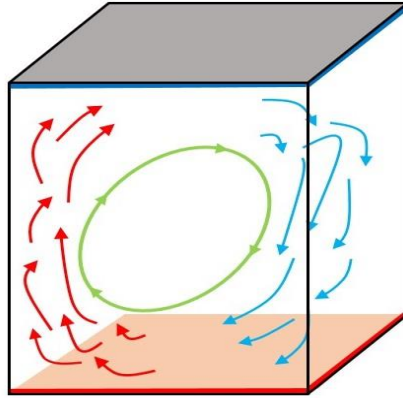


Figure 1. Sketch of a Rayleigh-Bénard convection cell.

In this system, initially the temperature distribution in the bulk of the fluid takes the shape of a linear gradient between the plates. When the temperature difference between both plates reaches a critical value, the buoyant forces overcome viscous forces in the fluid and the purely conductive heat transfer mechanism is replaced by a dynamic behavior, commonly in the form of a single circulating cell. Upon a further increase of the temperature difference between the plates the bifurcation phenomena begins to appear. The amount of circulating cells increases and a number of different and more complex flow patterns, referred here as dynamic states, can be obtained depending on the system conditions and geometry. The geometry of the system will determine indeed the amount of circulation cells that it can fit. A preferential dimension will be able to hold a larger amount of cells, for this reason the bifurcation points and the characteristics of the arising dynamic states are highly dependent on the geometry of the system.

Another important feature of this configuration is the occurrence of hysteresis, observed between the transitions from one state to the other [12], displaying several dynamic states for a given set of conditions, being these states reachable according to the departure from different initial conditions (IC) of the system.

3. NUMERICAL FORMULATION

To study the Rayleigh-Bénard convection case, a simple geometry consisting in a rectangular section cavity. For this type of geometry the main dimensionless parameters that govern the system dynamics are: (a) the aspect ratio A , defined as the ratio between the height (H) and width (W) or depth (D) of the cavity, and (b) the Rayleigh number Ra , which is the analogy of the Reynolds number for the cases of free convection, defined as:

$$Ra = \frac{g\beta\Delta TH^3 Pr}{\nu^2} \quad (13)$$

where g is the gravity acceleration, β is the thermal expansion coefficient, ΔT is the temperature difference between the plates, L is the characteristic dimension of the system, in this case the height, Pr is

the Prandtl number and ν is the kinematic viscosity. The value of Ra for which the stagnation condition is surpassed is known as critical Ra .

In the present work, a geometry with the height as the dominant direction was selected. This choice was made because this parameter is also expected to be adjustable in DHRS applications and because being the buoyant forces the principal driver of the dynamic of the system, a higher geometry has a potentially larger driving force.

It is important to note that both preliminary simulations and results extracted from the literature showed that 3D cases exhibit a behavior with a higher degree of complexity than the aimed for an initial assessment, even with a configuration as simple as the current one; that is idealized boundary conditions, a simple geometry and simplified heating and cooling schemes. In order to focus the efforts in the assessment and enhancement of the different numerical tools, geometry of the Rayleigh-Bénard convection flow was simplified to a 2D scheme and the values of Ra were maintained within the range corresponding to a laminar regime. The final geometry considered for this work is depicted in Fig. 2.

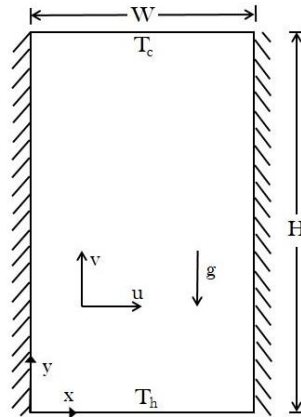


Figure 2. Sketch of the geometry used for the study cases.

3.1. Numerical Schemes and Procedure

A detailed modeling of the system was carried out for values of Ra and A in the range $[1.0 \cdot 10^4; 5.0 \cdot 10^6]$ and $[2; 4]$ respectively. For each value of A , this was done by simulating the evolution of the system for progressive step changes of Ra , both in the increasing and decreasing directions. Therefore, for a given set of initial condition the simulation was carried out until a final solution was obtained, either steady or oscillatory. Then by varying the value of Ra by a prescribed step size ΔRa , and repeating the entire process until the whole range of Ra was covered. A smaller value of ΔRa was used in the vicinity of the bifurcation points to accurately determine its position.

The numerical simulations of the system were carried-out using the OpenFOAM Computational Fluid Dynamics (CFD) libraries. The pressure-velocity coupling is handled by using the PIMPLE algorithm implemented within OpenFOAM, which is a combination of the PISO and SIMPLE algorithms for the description of temporal evolution of the flow. A second-order backward scheme was used for time stepping, with uniform steps. Under-relaxation was set to ensure the convergence of the iterative procedure. The computational spatial domain was covered with an orthogonal non-uniform grid, with higher refinement near the boundaries of the cavity, and a uniform spacing in the central region of the

cavity. For achieving the different values of A , the width of the cavity has been maintained constant while using the height as a control parameter. For each case the selected mesh is composed by $A \cdot 10^4$ rectangular cells. Within each time step, the spatial solution were considered to be fully converged when a prescribed tolerance value for the residuals associated to each variable is reached, namely $1 \cdot 10^{-7}$ for the velocity and temperature and $5 \cdot 10^{-7}$ for the pressure. Time-integration is stopped once an asymptotic solution, either stationary or periodic, is reached.

4. PERFORMANCE VERIFICATION

Before implementing the methodology for the analysis of the natural circulation, a performance verification of the accuracy of numerical simulations is needed, both concerning the description of the natural circulation system and the stability analysis procedure. For these purposes, the tools were assessed against different numerical benchmarks that resemble the behavior of our study case.

4.1. Natural Circulation Performance

For the assessment of the performance of the description of the natural circulation phenomena the selected case is the differentially heated cavity; a square 2D cavity heated and cooled from the opposing vertical walls and with adiabatic conditions for the horizontal ones [11]. While this case is not a configuration exhibiting the Rayleigh-Bénard convection that will be used in the present work, the similarities both in the simplicity of the geometry and the driving force governing the whole dynamic deems it sufficient for these means. The comparison is carried out for several values of Ra , within the constraints for maintaining a laminar regime; the velocity and temperature profiles are illustrated in Fig. 3 for the case of $Ra = 1.0 \cdot 10^5$.

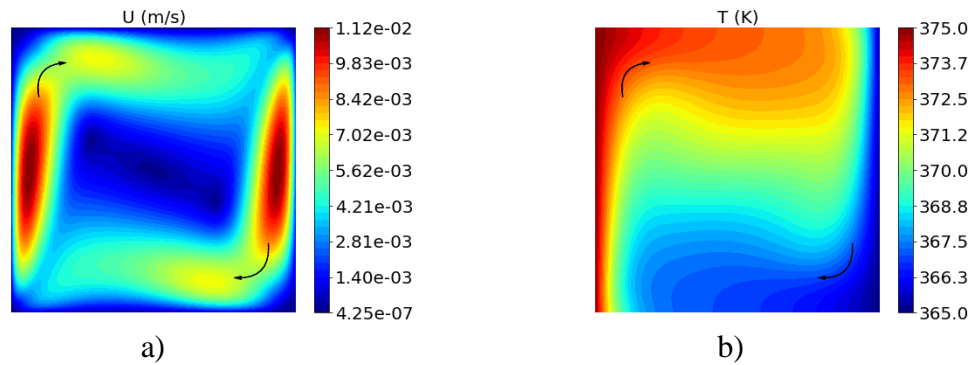


Figure 3. a) Velocity and b) Temperature profiles of the solution obtained for the differentially heated cavity case with $Ra = 1.0 \cdot 10^5$.

The parameters considered as a figure of merit are the average Nu number of the cavity and the maximum horizontal and vertical velocity components on the vertical and the horizontal midplane of the domain, respectively. The results obtained with the current model are presented in Table I, together with the corresponding to other studies found in the literature [11,12]. A very good agreement is observed with a relative error below 1% for all quantities. The values of velocity are presented in its dimensionless form for the sake of comparison.

Table I. Comparison of the reference dimensionless parameters for the differentially heated cavity case between the results from this work and studies found in literature .

Quantities	De Vahl Davis et al. [11]	D’Orazio et al. [12]	Present work
Ra = 1.0·10⁵			
U_{max}	3.649	3.650	3.654
V_{max}	3.697	3.695	3.690
Nu	1.118	1.119	1.113
Ra = 1.0·10⁶			
U_{max}	64.630	64.649	64.836
V_{max}	219.360	220.926	220.461
Nu	8.800	8.841	8.825

4.2. Stability Analysis Performance

With regard to the stability analysis tool an initial assessment has been carried out for the standard case of flow around a cylinder [13] with satisfactory results, but while this is a known case usually used for these means, this represents a forced convection case without the influence of buoyant forces, which is not representative of the key phenomena that is aimed to capture in this work, so it is omitted here for the sake of brevity. Instead, the study case corresponds to a similar configuration of the square 2D cavity used in the previous section, but replacing the adiabatic condition in the horizontal walls with a linear temperature profile between the values of the heated and cooled walls. For the assessment of the performance the figure of merit used corresponds to the characteristic frequencies derived from the eigenvalues of the linearized system. For this verification process, a study carried by Xin and Le Quére [14] is used. This study is based on an Arnoldi-iteration approach, particularly the Implicitly Restarted Arnoldi Method (IRAM), in contrast with the time-stepping approach used in the present work.

For the sake of comparison, specific values of parameters are used, specifically for the case of Rayleigh number $Ra = 4.05 \cdot 10^4$ and Prandtl number $Pr = 0.015$. The values of the frequencies derived from the leading eigenvalue obtained for the different methods are summarized in Table II, in their dimensionless form.

Table II. Comparison of the dimensionless frequency for $Ra = 4.05 \cdot 10^4$ with $Pr = 0.015$ computed in this work and the results from Xin and Le Quére [14]

Dimensionless frequency derived from the lead eigenvalue	IRAM Xin and Le Quére (2001)	Time-stepping and DMD (MATLAB®-OpenFOAM®)
$\hat{f}_i = \omega_i \cdot \frac{L^2}{2\pi\alpha\sqrt{Ra}}$	0.7123	0.7033

An additional verification study was carried against a similar study [15], with satisfactory results, but is omitted for the sake of brevity. The good agreement obtained with these comparisons show that the numerical tools used in this work have adequate accuracy to describe the dynamics of the configuration selected as a base case. In the next section, we will thus now describe the implementation of the methodology for the Rayleigh-Bénard convection flow case identified in section 3.

5. RESULTS

As mentioned previously, the behavior of the system is studied for conditions for which the stagnation has been overcome and a laminar flow regime has been established, which for the selected geometry corresponds to Ra values within the interval from $1.0 \cdot 10^4$ to $5.0 \cdot 10^6$.

Once the critical value of Ra is reached, the first dynamic state encountered corresponds to the classic solution of the Rayleigh-Bénard configuration depicted in Fig. 1: a single circulation cell covering the entirety of the cavity. As mentioned, the results presented here are obtained for geometries where the height is the dominant dimension, used as control variable to cover different values of A in the interval [2;4]. For cases within this range the geometry allows the allocation of an increasing number of smaller circulation cells. This way, for the case of $A = 2$, in the first bifurcation point the dynamic state evolves from the one-cell to a structure of two counter-rotating circulation cells, which is depicted in Fig 4.

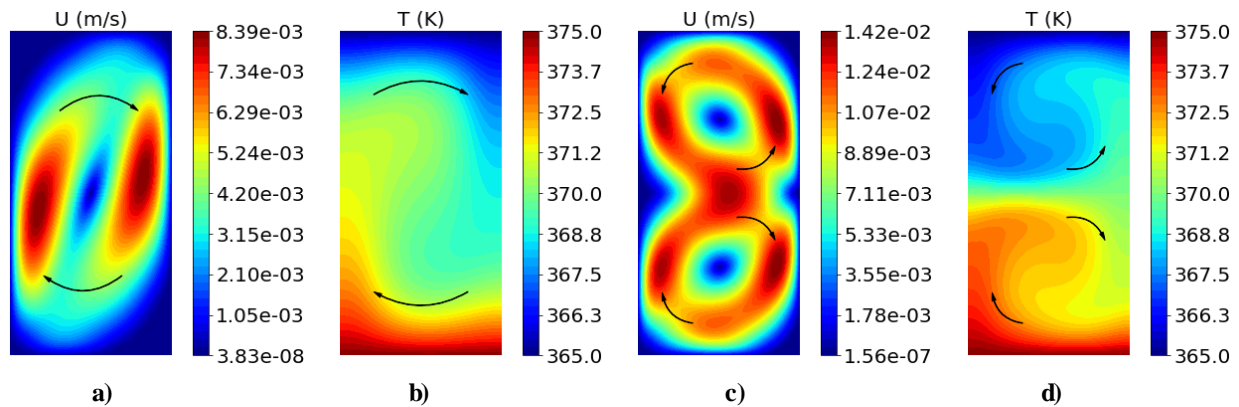


Figure 4. Velocity and Temperature profiles for different dynamic states. a) Velocity and b) Temperature profiles for the one-cell mechanism and c) Velocity and d) Temperature for the two-cells counter-rotating mechanism, for the aspect ratio of $A = 2$.

Typically, for steady-state solutions an increase in the number of cells involves a reduction on the overall heat removal capabilities of the system. This is explained by the fact that the path followed by the fluid from the bottom to the top regions becomes segmented. With the increase of the value of Ra , the intensity of these cells increases accordingly until at a given value the system begins to show an oscillating behavior in the relative intensity of the cells. The amplitude and frequency of these oscillations keeps increasing with the Ra until a new bifurcation point is reached: in this bifurcation point the behavior of the system shifts to a periodic dynamic state where new cells form in the corners of the cavity and then merge in the center of the cavity. The evolution of the velocity field for this type of behavior is illustrated in Fig. 5 for an aspect ratio of $A = 2.5$. In this case the depicted dynamic state begins with a single cell extended in the whole cavity, followed by two smaller cells forming in opposite corners. These new cells grow in size and intensity while the initial cell shrinks until its disappearance, leaving place for the new cells to continue growing and eventually merge into one single cell, restarting the cycle. This type of behavior has a positive impact in the heat transfer capabilities of the system as the velocity pattern is no longer segmented and a continuous mixing of the fluid is carried out.

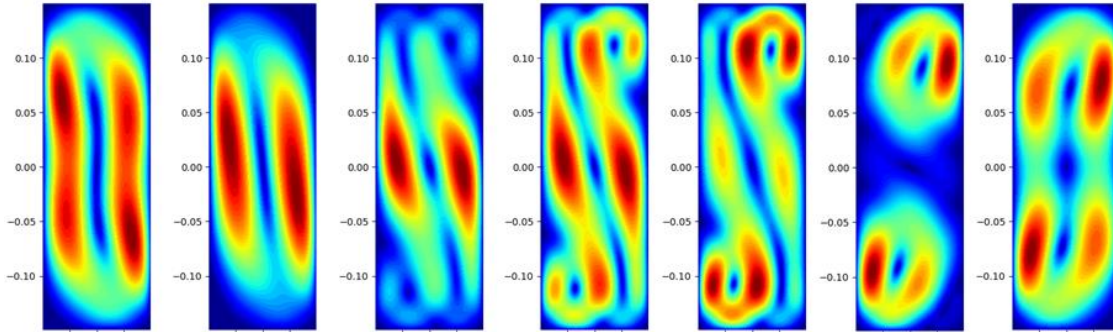
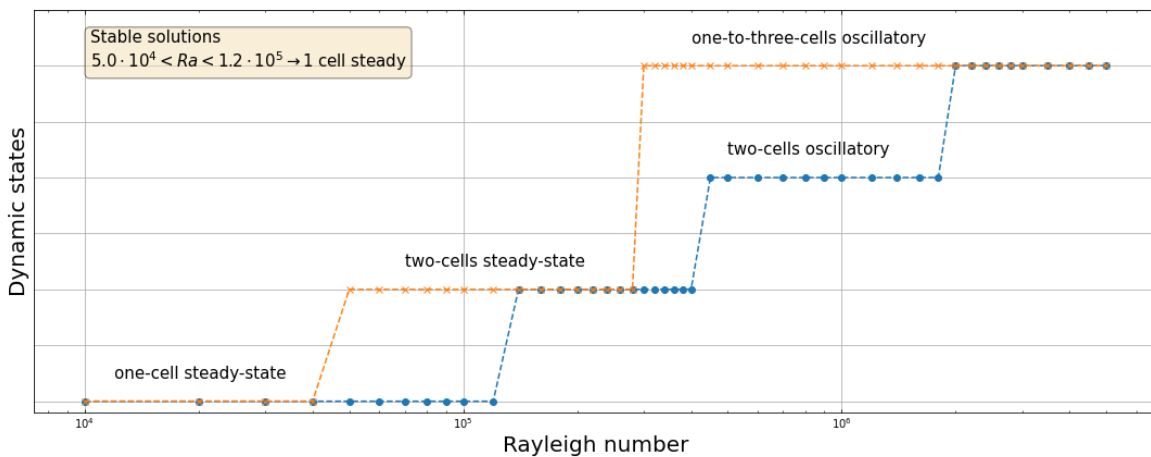


Figure 5. Evolution of the velocity field for the case $A = 2.5$ exhibiting a dynamic state with a cell creation-merging mechanism.

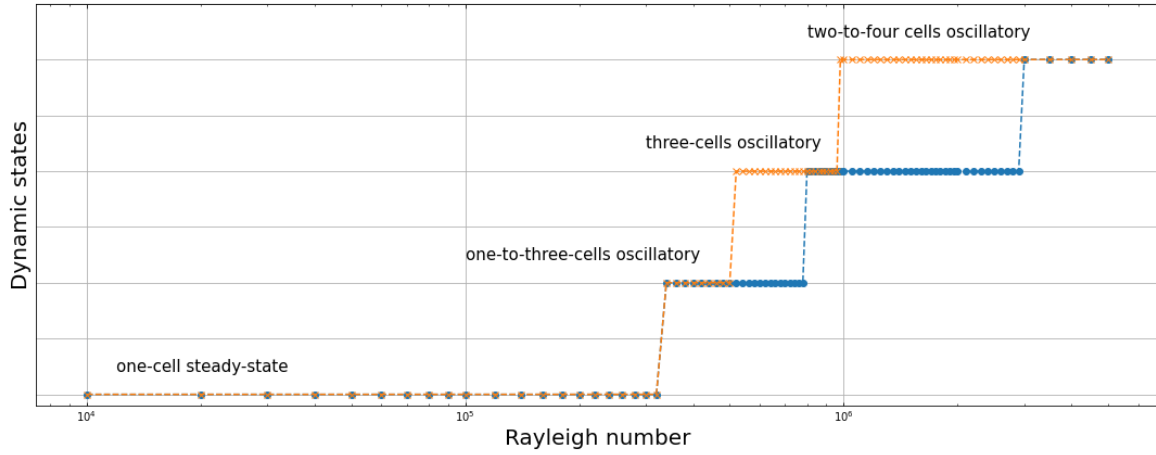
Further dynamic states are observed for higher values of A but with similar mechanisms: a constant amount of cells with either steady or oscillating asymptotic behaviors or a cyclic mechanism of cell creation-merging from the corner to the center of the cavity. For the largest value of A considered here a maximum of five simultaneous cells have been observed. Another important phenomenon observed in the simulations is that, as expected, a more elongated cavity requires a larger component of buoyant forces, this is, a larger value of Ra , to overcome the stagnated state.

It is also important to notice that the cases where the amount of circulation cells does not change over time have an additional bifurcation. Given the fact that the geometry does not provide a preferable sense of circulation, both of the mirrored solutions are equally feasible.

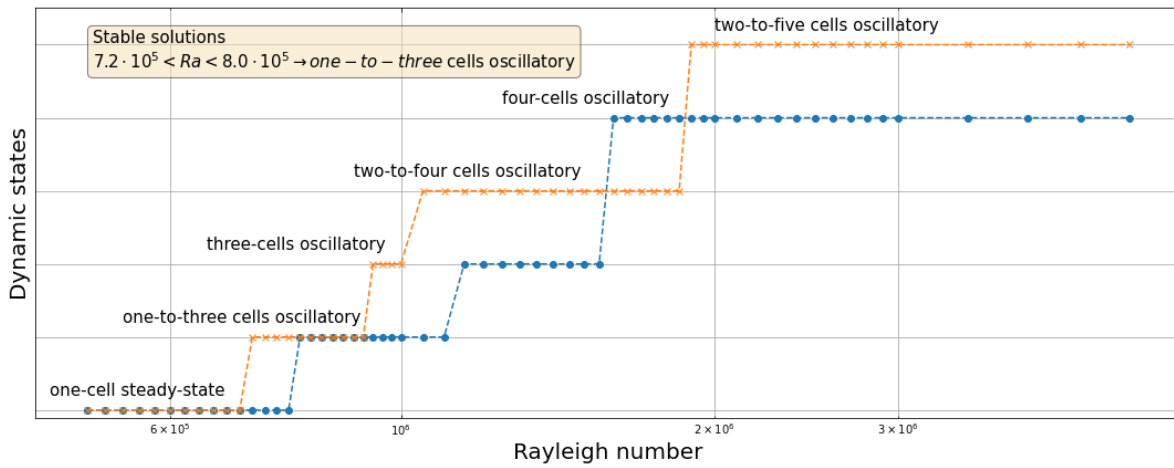
The existence of hysteresis in this system is illustrated by results obtained for both the cases of increasing and decreasing values of Ra , as can be seen in Fig.6. This figure presents the evolution of the dynamic states for the selected cases of $A = 2$, $A = 3$ and $A = 4$. This process aids the detection of the bifurcation phenomena since having a different set of ICs for each case allows obtaining the different coexisting solutions and its range of appearance, whereas the results in a single direction may not include all the dynamic states and only suggest the location of a bifurcation point. For example, in the Fig. 6a, the results for the increasing Ra case first exhibit the two-cell steady state solution for a value of $Ra = 1.4 \cdot 10^5$, while the results from the decreasing case allows to see that this dynamic state is achievable for values of Ra as low as $5.0 \cdot 10^4$.



a)



b)



c)

Figure 6. Evolution of the dynamic states for increasing (blue dots) and decreasing (orange crosses) step changes of Ra. a) $A=2$, b) $A=3$ and c) $A=4$. The range of Ra is adjusted to the region of interest of the different cases. The stability analysis is carried out for the steady-state solutions.

As mentioned before, an important aspect to point out is that the procedure for finding the different dynamic states, this is, studying the evolution of the system for an increase and decrease of Ra number, is deemed sufficient for the case selected in this work, but this is related to its overall complexity and availability of results, and does not ensure its applicability for a more complex case.

Once all the possible dynamic states of the system and their range of appearance are known, for a complete description of the evolution their stability must be addressed, particularly for the ranges in which two different solutions coexist.

As discussed in section 2.2, the method used to do this is based on a linear stability analysis considering small perturbations around the steady-state solution of the system. This type of approach excludes the analysis of cases with an oscillating asymptotic solution, since it is not possible to capture the dynamic of the temporal variation of an oscillatory base solution.

The analysis was carried out as follows; for the ranges in which both the increasing and decreasing cases were in accordance, this is, where a single solution was found, it is directly considered as stable. For the

ranges with two coexisting solutions, the analysis was carried out where it was possible. This means, over the cases with steady-state base solution, in this way if a steady-state and an oscillatory solution are coexisting, the conclusion is drawn from the analysis of the former. In this situation the oscillatory solution is considered to be stable only if the remaining one is not. Finally for the cases where two oscillatory solutions coexist, no conclusion about its stability can be drawn with the method presented here. The stability is determined from the study of the eigenvalues retrieved from the evolution of the linearized system. In Fig. 6, for each case the stable solution is indicated for the ranges in which is possible. It can be observed that these constraints of the current method rule-out the stability analysis of a significant portion of the results of this study, especially for the cases with $A = 3$ where the only coexisting solutions are oscillatory, pointing out the need to extend to current capabilities to achieve an integral analysis of the behavior of the system.

Among the different cases the general behavior of the system can be divided between the initial behavior based in the single cell solution, with good heat transfer capabilities and covering a range in which is either the only or the most stable solution, but with limitations in the maximum value of Ra , against the behavior for higher values of Ra that is characterized by the coexistence of oscillatory states, with an occurrence highly dependent on the specific conditions. This study is not representative of the final configurations of the possible applications, so no conclusions can be drawn about which one of these behaviors is preferred.

Finally, the results of the different cases are used to build a single bifurcation diagram covering the whole range of parameters studied. This allows illustrating how the dynamic state of the system changes as a function of both the geometric and the physical parameters. This diagram is presented in Fig. 7, where each point corresponds to change in the dynamic state of the system, associated with a bifurcation point. Diagrams were obtained for both increasing and decreasing values of Ra , but only the corresponding to the decreasing case is presented for the sake of brevity. For the values of $A = 2, 3$ and 4 , the points correspond to the changes of dynamic state presented in Fig. 6.

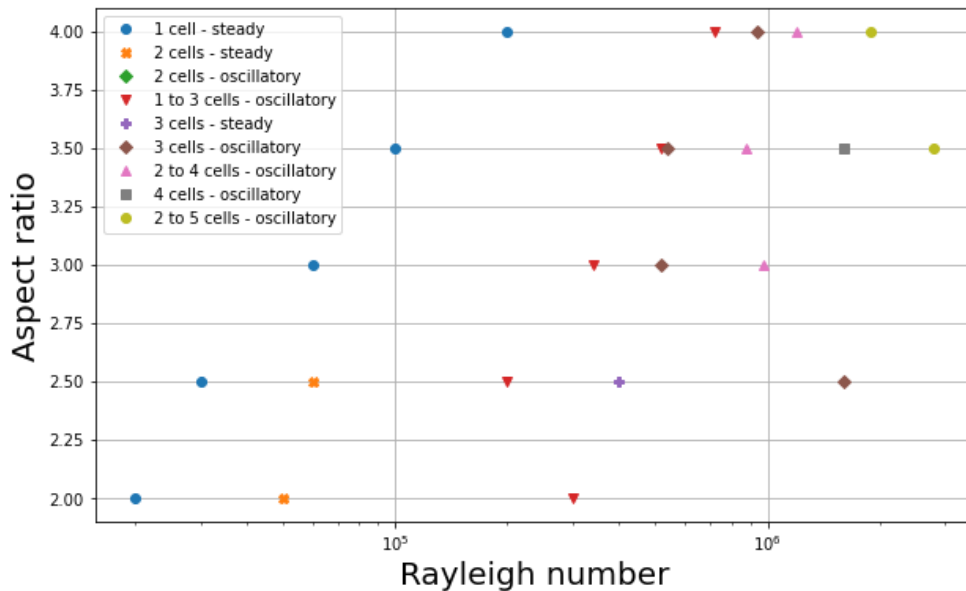


Figure 7. Bifurcation diagram for the case of decreasing Ra . Each point indicates a change in the dynamic state of the system, meaning that such solution is maintained for higher values of Ra until the next point is encountered.

From this diagram can be observed that the majority of the dynamic states are, as expected, concentrated for higher values of both Ra , since for higher contributions of the buoyant forces the division into smaller cells is enhanced, and A , since the maximum amount of cells and therefore of different dynamic states is limited by the relative height of the cavity.

6. CONCLUSIONS AND FUTURE WORK

The present work poses a starting point for the development of a methodology for assessing the performance of molten salt natural circulation systems. The main constraints for the method were discussed and a base study case was selected from the available literature. For the early development of this procedure a very simple case has been used, focusing in the fundamental capabilities of the tool and the method. The initial implementations have been carried out successfully, with a proper verification of the performance of the numeric tool against different benchmarks taken from the literature, and other studies covering the Rayleigh-Bénard convection case [11-15]. The results obtained allow highlighting the need for this kind of analysis tool; when reducing the problem to almost one of the simplest configurations, as it is a simple 2D geometry working in a laminar regime, the degree of complexity that arises and the diversity of the results requires a set of different models that will only continue to increase as the studied cases are closer to a realistic system. One can cite for example, the addition of turbulence modeling, molten salt specific phenomena, 3D geometries and realistic boundary conditions. For this kind of analysis to be feasible at the design stage of systems and components where a large number of different configurations may be considered, the methodology requires an optimal combination of the existing tools for each one of the required steps. The applicability of the current implementation to increasingly complex cases, where the contribution of turbulence and 3D geometries, to mention a few, begins to be significant is currently being investigated.

The first problem to be addressed is the computational cost of carrying out the required amount of simulations, this is, the need to include an alternative to the use of full order models to be able to make an analysis in a sufficiently short time scale. While this has not been a limiting factor for the results presented here, the computational cost for more complex cases will deem the current approach as unfeasible. On this behalf the application of Reduced Order Models for the bifurcation problem is being investigated. Secondly, the procedure used for the detection of the bifurcation points is based on the fact that different ICs may lead to different dynamic states, due the highly non-linear characteristic of the natural circulation systems. The approach used in this work is systematic but limited in the amount of different ICs taken into account. With a reduction in the computational cost this could be extended for more complex cases to ensure the description of all the possible dynamic states.

Finally, due to the foreseen application in the nuclear safety systems, the initial capabilities of the tool tend to rule out all the non-steady solutions out of the stability analysis, regarding them as uninteresting for being unfeasible under ideal conditions for the desired applications. However, the obtained results show that the majority of the possible solutions showed in some extent an oscillating behavior that does not necessarily causes a detriment in the heat transfer capabilities of the overall system. In addition, this state could not be avoided under abnormal conditions and thus the stability analysis needs to be extended for the cases where the base solution of the system is a non-steady one.

ACKNOWLEDGMENTS

This project has received funding from the Euratom research and training programme 2014-2018 under grant agreement no. 847527. The data that support the findings of this study are openly available in Zenodo at <http://doi.org/10.5281/zenodo.5786092>.

REFERENCES

1. DOE, U. S. A technology roadmap for generation IV nuclear energy systems. <https://www.hsd.org/?view&did=894>, 2002.
2. Serp, J., Allibert, M., Beneš, O., Delbec, S., Fevberg, O., Ghetta, V., & Zhimin, D. "The molten salt reactor (MSR) in generation IV: overview and perspectives". *Progress in Nuclear Energy*, **77**, 308-319. (2014).
3. Retamales, M. T. Development of multi-physical multiscale models for molten salts at high temperature and their experimental validation (Doctoral dissertation, Université Grenoble Alpes). (2018).
4. Gérardin, D., Allibert, M., Heuer, D., Laureau, A., Merle-Lucotte, E., & Seuvre, C. "Design evolutions of the molten salt fast reactor". *International Conference on Fast Reactors and Related Fuel Cycles: Next Generation Nuclear Systems for Sustainable Development (FR17)*, Yekaterinburg, Russia, June 26–29, 2017 (2017).
5. INTERNATIONAL ATOMIC ENERGY AGENCY, "Natural Circulation in Water Cooled Nuclear Power Plants", *IAEA-TECDOC-1474*, IAEA, Vienna (2005).
6. Strogatz, S. H. *Nonlinear dynamics and chaos with student solutions manual: With applications to physics, biology, chemistry, and engineering*. Chapter 3. CRC press, Boca Raton, Florida, USA (2018).
7. Jasak, H., Jemcov, A., & Tukovic, Z. OpenFOAM: A C++ library for complex physics simulations. *International workshop on coupled methods in numerical dynamics*. **Vol. 1000**, pp. 1-20. IUC Dubrovnik Croatia. (2007, September).
8. Lyapunov, A. M. "The general problem of the stability of motion". *International journal of control*, **55**(3), 531-534. (1992).
9. Theofilis, V. "Global linear instability". *Annual Review of Fluid Mechanics*, **43**, 319-352. (2011).
10. Pini, A., Cammi, A., Lorenzi, S., Cauzzi, M. T., & Luzzi, L. "A CFD-based simulation tool for the stability analysis of natural circulation systems." *Progress in Nuclear Energy*, **117**, 103093. (2019).
11. de Vahl Davis, G. "Natural convection of air in a square cavity: a bench mark numerical solution." *International Journal for numerical methods in fluids*, **3**(3), pp 249-264. (1983).
12. D'Orazio, M. C., Cianfrini, C., & Corcione, M. "Rayleigh-Bénard convection in tall rectangular enclosures." *International journal of thermal sciences*, **43**(2), pp 135-144. (2004).
13. Giannetti, F., & Luchini, P. "Structural sensitivity of the first instability of the cylinder wake." *Journal of Fluid Mechanics*, **581**, pp 167-197. (2007).
14. Xin, S., & Le Quéré, P. "Linear stability analyses of natural convection flows in a differentially heated square cavity with conducting horizontal walls." *Physics of Fluids*, **13**(9), pp 2529-2542. (2001).
15. Merzari, E., Fischer, P., & Pointer, W. D. "Optimal disturbances in three-dimensional natural convection flows". *Fluids Engineering Division Summer Meeting*, **Vol. 44755**, pp. 921-928. American Society of Mechanical Engineers. (2012, July).